DESY 99-005
MPI/PhT/99-002

DESY 99–005
MPI/PhT/99–002
hep–ph/9901348
January 1999

ISSN 0418–9833

Inclusive J/ψ and $\psi(2S)$ Production from B Decay in $p\bar{p}$ Collisions

B.A. Kniehl[1] and G. Kramer[2]
[1] Max-Planck-Institut für Physik (Werner-Heisenberg-Institut),
Föhringer Ring 6, 80805 Munich, Germany
[2] II. Institut für Theoretische Physik*, Universität Hamburg,
Luruper Chaussee 149, 22761 Hamburg, Germany

hep-ph/9901348 19 Jan 1999

Abstract

Using information on B-meson fragmentation functions from CERN LEP 1 and adopting the nonrelativistic QCD factorization formalism proposed by Bodwin, Braaten, and Lepage, we predict the transverse-momentum distribution of J/ψ mesons originating from the inclusive decays of b hadrons produced in $p\bar{p}$ collisions at the Fermilab Tevatron. We determine the relevant colour-octet charmonium matrix elements from fits to CDF data on prompt charmonium hadroproduction and to CLEO data on charmonium production from B-meson decay. Our predictions are found to agree well with recent CDF and D0 data.

PACS numbers: 13.60.-r, 13.85.Ni, 13.87.Fh, 14.40.Lb

*Supported by Bundesministerium für Bildung, Wissenschaft, Forschung und Technologie (BMBF), Bonn, Germany, under Contract 05 7 HH 92P (0), and by EU Fourth Framework Programme *Training and Mobility of Researchers* through Network *Quantum Chromodynamics and the Deep Structure of Elementary Particles* under Contract FMRX–CT98–0194 (DG12 MIHT).

1 Introduction

Recently the production of J/ψ and ψ'[1] mesons in $p\bar{p}$ collisions at $\sqrt{s} = 1.8$ TeV was studied with the CDF detector at the Fermilab Tevatron [1]. The J/ψ and ψ' mesons were reconstructed from their $\mu^+\mu^-$ decay modes. The inclusive production cross sections for both charmonium states were measured as functions of the transverse momentum (p_T) in the central region, corresponding to the rapidity (y) range $|y| < 0.6$. The CDF Collaboration was able to extract individual cross sections for J/ψ and ψ' mesons originating from weak decays of b hadrons and from prompt production. In this way, rather accurate data for the inclusive J/ψ and ψ' cross sections coming from the decays of B mesons or other hadrons containing b quarks were obtained for p_T values between 5 and 20 GeV. These cross sections were compared with theoretical predictions based on next-to-leading (NLO) calculations in quantum chromodynamics (QCD) with massive b quarks [2] and subsequent fragmentation of the b quarks into b hadrons. The b-hadron decays to $J/\psi + X$ and $\psi' + X$ were described by a parametrization of the momentum distribution measured by the CLEO Collaboration [3]. It was found that the data for J/ψ (ψ') production were higher than the QCD prediction by a factor of 2–4 (3–4) depending on the p_T of the J/ψ (ψ') meson. However, for larger p_T values, *i.e.* $p_T \gtrsim 12$ GeV, the experimental cross sections could be reproduced by the theoretical calculations if the scale μ, the b-quark mass m_b, and the parameter ϵ in the Peterson [4] fragmentation function (FF) were simultaneously reduced from $\mu = m_T = \sqrt{p_T^2 + m_b^2}$ to $\mu = m_T/4$, from $m_b = 4.75$ GeV to $m_b = 4.5$ GeV, and from $\epsilon = 0.006$ to $\epsilon = 0.004$, respectively. Even with this choice of parameters, the measured cross section for J/ψ production was still a factor of 2 above the prediction at $p_T \lesssim 6$ GeV. In the case of ψ' production, the cross section predicted with the modified parameters is still below the data, although the discrepancy was only about one standard deviation at large p_T.

For the nominal J/ψ and ψ' predictions, it was assumed that the nonperturbative part of the fragmentation of b quarks into b hadrons can be described by a Peterson FF with $\epsilon = 0.006$. This value for ϵ was extracted more than ten years ago from a global analysis of data on B production in e^+e^- annihilation at PETRA and PEP [5], based on Monte Carlo (MC) models which were in use at that time. Due to the nonperturbative nature of the Peterson FF, the choice of ϵ must be backed up by other independent data, *e.g.* on $e^+e^- \to B + X$, which must be analysed within the very theory that is used for the interpretation of the CDF data, *i.e.* NLO QCD with massive quarks ($m_b \neq 0$) and fixed order in α_s (massive scheme [6]). In e^+e^- annihilation, this theory is only reliable just above threshold, where almost no data exist, except from the ARGUS and CLEO experiments at the $\Upsilon(4S)$ resonance. In this case, however, the B mesons are only produced in pairs and not in the fragmentation mode. Therefore, the underlying description of $b \to B$ fragmentation in the massive scheme, on which the comparison with the CDF data is based, is to a large extent *ad hoc* and not supported by the analysis of independent data within the same NLO perturbative scheme. Reliable information on

[1] We denote the $\psi(2S)$ meson by ψ'.

the FF for b hadrons can only be gained from the high-statistics experiments at CERN LEP 1. At LEP 1, the production of b quarks is enhanced as compared with the lower e^+e^- energies, so that the produced b hadrons can be identified more easily through their weak decays. The fragmentation into B mesons was measured by the OPAL Collaboration at LEP 1 [7]. Based on these data, we recently constructed FF's for B mesons using three different forms for the FF at the starting scale μ_0, including the one by Peterson *et al.* [4], which yielded the lowest χ^2 values at leading order (LO) and NLO [8].

In Ref. [8], the $b \to B$ FF was obtained using the so-called massless scheme [6]. In this scheme, the parton-level cross sections are calculated with $m_b = 0$, and the appearing collinear final-state singularities are factorized into the FF's according to the modified minimal-subtraction ($\overline{\rm MS}$) scheme. A nonvanishing value for m_b only appears in the initial conditions for the FF's. This scheme provides the appropriate approach for describing the fragmentation of b quarks into B mesons at the Z-boson resonance, since the b quarks in the reaction $e^+e^- \to b\bar{b} \to B + X$ typically have large momenta. A large-momentum b quark essentially behaves like a massless particle, radiating a large amount of its energy in the form of hard, collinear gluons. This leads to the well-known logarithms of the form $\alpha_s \ln(M_Z^2/m_b^2)$ originating from collinear radiation in a scheme where m_b is taken to be finite. These terms appear in all orders of perturbation theory. The method for summing them is to introduce FF's and to absorb the m_b-dependent logarithms into their evolution up to the factorization scale of order M_Z. If all terms of $\mathcal{O}(m_b^2/M_Z^2)$ are neglected and the $\overline{\rm MS}$ subtraction scheme is adopted, then this approach is equivalent to the massless scheme, where one puts $m_b = 0$ from the beginning. In the massless scheme, a nonperturbative FF is easily incorporated. This allows one to transfer the information on the fragmentation process in one reaction to other processes, *e.g.* $p\bar{p} \to B + X$. This was done in Ref. [8], where the b-quark FF's obtained from fits to the OPAL data were used to predict the differential cross section $d\sigma/dp_T$ of B production in $p\bar{p}$ scattering at $\sqrt{s} = 1.8$ TeV. These predictions were compared with data from the CDF Collaboration [9] and found to agree with them within errors. In this paper, we use these results for B production to predict the distribution $d\sigma/dp_T$ of J/ψ and ψ' mesons originating from b-hadron decay. For this purpose, we need a realistic description of the inclusive B decays into J/ψ and ψ' mesons. We adopt the parton-model description from Ref. [10], which allows one to nicely interpret the CLEO data [3].

While only B^+ and B^0 mesons and their antiparticles, which we collectively call B mesons in the following, are produced at CLEO energies, the CDF J/ψ and ψ' samples also contain contributions from B_s mesons, B_c mesons, Λ_b baryons, etc. We may safely ignore B_c production, whose rate is expected to be about 10^{-3} of the total b-hadron production rate [11]. The c quark in the initial state should enhance the branching ratio to charmonium, but B_c production is expected to account for $\lesssim 1\%$ of all events of charmonium production from b-hadron decay at the Tevatron [12]. Unfortunately, there exist no measurements of the differential cross sections of B_s and Λ_b production at LEP 1, which could be used to extract FF's for these hadrons. Moreover, there are no data on the momentum distributions of the J/ψ and ψ' mesons inclusively produced in B_s and Λ_b decays. Only the branching fractions of $b \to \bar{B}_s$ and $b \to \Lambda_b$ (here Λ_b stands for a

collection of b baryons) are known, which are approximately 10% each [13]. Thus, the dominant channels for b-quark fragmentation are $b \to B^-$ and $b \to \bar{B}^0$. Due to the lack of detailed knowledge of the fragmentation into B_s mesons and Λ_b baryons and their inclusive J/ψ and ψ' decay properties, we must estimate the B_s and Λ_b contributions using information on $b \to B$ fragmentation and on the momentum distributions of the inclusive $B \to J/\psi + X$ and $B \to \psi' + X$ decays. For simplicity, we assume that the $b \to \bar{B}_s$ and $b \to \Lambda_b$ FF's are proportional to those of $b \to B^-$ [8], and scale the latter by the factor $B(b \to \bar{B}_s)/B(b \to B^-)$ and similarly for $b \to \Lambda_b$ adopting the values for these branching ratios from Ref. [13]. Furthermore, we approximate the momentum distributions of the J/ψ (ψ') mesons from the B_s and Λ_b decays by the one of $B \to J/\psi + X$ ($B \to \psi' + X$).

This paper is organized as follows. In Sect. 2, we recall the framework for calculating the cross section of B production in $p\bar{p}$ collisions closely following our earlier work [8]. In Sect. 3, the momentum distributions of J/ψ, χ_{cJ}, and ψ' mesons from B decay, which enter the predictions of charmonium production from b-hadron decay at the Tevatron, are described in the framework of nonrelativistic QCD (NRQCD) [14]. In Sect. 4, the relevant charmonium matrix elements are determined from CDF [1] and CLEO [3] data on prompt charmonium production. In Sect. 5, we calculate the p_T spectra of J/ψ and ψ' mesons originating from b-hadron decay at the Tevatron and compare them with available CDF [1] and D0 [15] data. Section 6 summarizes our conclusions.

2 B-meson production in $p\bar{p}$ collisions

In Ref. [8], we presented LO and NLO predictions for the inclusive cross section of B production in $p\bar{p}$ collisions with $\sqrt{s} = 1.8$ TeV at the Tevatron. This analysis provides the basis for the theoretical description of the inclusive production of J/ψ and ψ' mesons from b hadrons at the Tevatron. Having obtained the inclusive B cross section $d\sigma/dp_T$, this cross section is convoluted with the appropriately boosted longitudinal-momentum distributions of the J/ψ and ψ' mesons from B decay, which are considered in the next section. In this way, we obtain the bulk of the cross section, more than 80% of it, from which the additional contributions originating from the production of B_s mesons and Λ_b baryons may be estimated.

Before we come to these points, we shortly recapitulate the input that was assumed in Ref. [8]. The formalism used in Ref. [8] is very similar to Ref. [16], where inclusive light-meson production in $p\bar{p}$ collisions was studied in the QCD-improved parton model. We work at NLO in the $\overline{\rm MS}$ scheme with $N_f = 5$ massless flavors. In this respect, we differ from any of the massive calculations [2], where only $N_f = 4$ active flavors are taken into account. For the proton and antiproton parton density functions (PDF's) we use the set CTEQ4M [17] with asymptotic scale parameter $\Lambda^{(5)}_{\overline{\rm MS}} = 202$ MeV or the more recent set MRST [18] of the Durham-Oxford-Rutherford group with $\Lambda^{(5)}_{\overline{\rm MS}} = 211$ MeV, which corresponds to $\Lambda^{(4)}_{\overline{\rm MS}} = 300$ MeV and a b-quark mass of $m_b = 4.3$ GeV [18]. The authors of Ref. [18] presented new fits to the relevant deep-inelastic-scattering data incorporating a more realistic description of the heavy-quark PDF's, with an improved extrapolation from

scales near threshold to higher scales. For the B FF's, we adopt set NLO P [8], which uses the Peterson form [4] for the $b \to B$ FF at the initial scale and yielded the best fits to the OPAL data [7]. The two alternative sets S and B, which are provided in Ref. [8], lead to almost identical predictions for inclusive B hadroproduction. The evolution of the FF's is performed with $\Lambda^{(5)}_{\overline{\rm MS}} = 227$ MeV [8]. The strong coupling constant $\alpha_s^{(5)}(\mu)$ is evaluated from the two-loop formula adopting the $\Lambda^{(5)}_{\overline{\rm MS}}$ value from the selected set of proton PDF's. We identify the factorization scales associated with the proton, antiproton, and B meson and collectively denote them by M_f. We choose the renormalization and factorization scales to be $\mu = M_f = 2\xi m_T$, where ξ is a number of order unity and $m_T = \sqrt{p_T^2 + m_\psi^2}$ is the transverse mass of the produced charmonium state, which we generically denote by ψ. Unless otherwise stated, we put $\xi = 1$. We recall that, in the case of inclusive B production discussed in Ref. [8], we instead took m_T to be the B transverse momentum. In the present case, we consider it more appropriate to relate m_T to the final-state ψ state. The rationale is that we combine the $b \to B$ fragmentation and $B \to \psi + X$ decay processes into one single process. This scale convention also considerably simplifies the computations, since the evolution of the B FF's are performed numerically in x space [19]. Later on, we study the scale dependence of our results in order to get some handle on the theoretical uncertainty related to this arbitrariness in convention. We adopt all kinematic conditions from Ref. [1].

When we present LO results, they are consistently computed using set CTEQ4L [17] (MRSTLO [18]) of proton PDF's, set LO P of B FF's [8], the one-loop formula for $\alpha_s^{(5)}(\mu)$ with $\Lambda^{(5)} = 181$ MeV [17] ($\Lambda^{(5)} = 132$ MeV [18]) and the LO hard-scattering cross sections.

3 Charmonium production from B-meson decay

The inclusive decay $B \to J/\psi + X$ has three sources: the prompt production of J/ψ mesons and the two feed-down modes $B \to \psi' + X$ followed by $\psi' \to J/\psi + X$ and $B \to \chi_{cJ} + X$, with $J = 0, 1, 2$, followed by $\chi_{cJ} \to J/\psi + \gamma$. In the recent CLEO measurements [3], these three sources were disentangled and found to have the branching fractions $(0.80 \pm 0.08)\%$, $(0.19 \pm 0.03)\%$, and $(0.13 \pm 0.02)\%$, respectively. The total inclusive J/ψ branching fraction was measured to be $B(B \to J/\psi + X) = (1.12 \pm 0.07)\%$ [3]. The inclusively produced ψ' mesons are all believed to be promptly produced. The CLEO Collaboration also measured the momentum distribution of the $B \to J/\psi + X$ decay including all three sources and the one of the $B \to \psi' + X$ decay. Furthermore, they presented the momentum distribution of the prompt $B \to J/\psi + X$ decay, *i.e.* with the contributions due to the two feed-down channels subtracted.

In order to predict the inclusive cross section of J/ψ mesons from B decay in $p\bar{p}$ collisions, we need the total J/ψ momentum distribution, *i.e.* the sum of the prompt and the two feed-down contributions. So, the easiest way to incorporate the CLEO information would be to boost back the CLEO data, measured in the CLEO laboratory frame, into the B rest frame. In this system, the distribution is assumed to be isotropic. This distribution must then be boosted from the B rest frame along the momentum direction of

the produced B meson to the Tevatron laboratory frame. This procedure can easily be implemented into an event generator to be used for the analysis of the experimental data [1]. Our procedure of incorporating the CLEO information is somewhat different. We first calculate, within NRQCD [14], the momentum distribution of J/ψ mesons promptly produced from B decay in the B rest system. From this we derive the longitudinal-momentum distribution of the J/ψ mesons for B mesons in flight by performing an appropriate boost and integrating over the transverse momentum components. To adjust the input parameters, the momentum distribution in the B rest system is boosted to the CLEO laboratory frame and compared with the CLEO data. This already accounts for 71% of the J/ψ mesons coming from B decay. The same procedure can be applied to the $B \to \psi' + X$ decay mode. As we shall see in Sect. 4, in the case of $B \to \chi_{cJ} + X$, the NRQCD prediction falls short of the CLEO data [3], so that its normalization must be adjusted by hand. For simplicity, the feed-down from ψ' and χ_{cJ} mesons to J/ψ mesons is accounted for by including the respective branching fractions and assuming that the J/ψ mesons receive the full momentum of the primary charmonium states.

The momentum spectrum of the prompt, inclusive $B \to J/\psi + X$ decay has been investigated just recently by Palmer, Paschos, and Soldan [10] in the NRQCD approach [14]. In this approach, the decay $b \to J/\psi + X$ is represented by a sum of products, each of which consists of a short-distance coefficient for the creation of a $c\bar{c}$ pair in a specific angular-momentum ($^{2S+1}L_J$) and color ($a = 1, 8$) configuration and a nonperturbative NRQCD matrix element $\left\langle \mathcal{O}^{J/\psi}[\underline{a}, {}^{2S+1}L_J] \right\rangle$, which parametrizes the subsequent evolution of the intermediate $c\bar{c}[\underline{a}, {}^{2S+1}L_J]$ state into the physical J/ψ state (plus light hadrons) via the emission of soft gluons. In their work, the transition $B \to b$ is described by two alternative models, the parton model and the model based on Fermi momentum smearing [20]. These models differ in the description of the long-distance transition $B \to b$. In the parton model approach, the transition $B \to b$ is parametrized by a distribution function similar to the one used in deep-inelastic scattering. In the Fermi motion approach, the bound-state corrections to the free-b-quark decay are incorporated by giving the spectator quark a Fermi motion inside the B meson. Since both models rely on unknown parameters, which are fixed by the CLEO data on the $B \to J/\psi + X$ prompt, inclusive decay, we expect that the fine details of describing the $B \to b$ transition are irrelevant for our purposes. In particular, as we shall see, the momentum distribution of the J/ψ mesons boosted to the Tevatron laboratory frame only depends on the bulk properties of the momentum distribution in the B rest system. In the following, we adopt the parton-model description of $B \to b$.

In the perturbative NRQCD framework, one first calculates the decay rate $\Gamma(b \to c\bar{c}[\underline{a}, {}^{2S+1}L_J] + q)$ of a b quark going to a $c\bar{c}$ pair in state $[\underline{a}, {}^{2S+1}L_J]$ plus a light quark q, where $q = d, s$. Then, one obtains from this the $b \to J/\psi + X$ decay rate by exploiting the NRQCD factorization theorem. In the b-quark rest frame, the final formula reads [10]

$$\Gamma(b \to J/\psi + X) = \frac{G_F^2}{144\pi} |V_{cb}|^2 m_c m_b^3 \left(1 - \frac{4m_c^2}{m_b^2}\right)^2 \left[a\left(1 + \frac{8m_c^2}{m_b^2}\right) + b\right], \qquad (1)$$

where G_F is Fermi's constant, V_{cb} is an element of the Cabibbo-Kobayashi-Maskawa ma-

trix, and a and b are NRQCD coefficients given by

$$a = (2C_+ - C_-)^2 \frac{\left\langle \mathcal{O}^{J/\psi}[\underline{1}, {}^3S_1] \right\rangle}{3m_c^2} + (C_+ + C_-)^2 \times \left[\frac{\left\langle \mathcal{O}^{J/\psi}[\underline{8}, {}^3S_1] \right\rangle}{2m_c^2} + \frac{\left\langle \mathcal{O}^{J/\psi}[\underline{8}, {}^3P_1] \right\rangle}{m_c^4} \right],$$
$$b = (C_+ + C_-)^2 \frac{\left\langle \mathcal{O}^{J/\psi}[\underline{8}, {}^1S_0] \right\rangle}{2m_c^2}. \tag{2}$$

Here, it is assumed that $m_q = 0$ and $|V_{cs}|^2 + |V_{cd}|^2 = 1$. $C_\pm$ are the short-distance coefficients appearing in the effective weak-interaction Hamiltonian that describes the $b \to c\bar{c}q$ transition. We observe that the $b \to J/\psi + X$ decay rate essentially depends on two parameters, a and b, which are given in terms of the charm-quark mass m_c, the short-distance coefficients $C_\pm$, and the NRQCD color-singlet and color-octet matrix elements. In our numerical analysis, we use $G_F = 1.16639 \cdot 10^{-5}$ GeV^{-2}, $V_{cb} = 0.0395$, $m_c = M_\psi/2$, where $M_\psi = 3.09688$ GeV [13] is the J/ψ mass, $C_+ = 0.868$, and $C_- = 1.329$ [10]. The NRQCD matrix elements are specified in Sect. 4.

The inclusive decay of the B meson is described by introducing the structure function $f(x)$ for the transition $B \to b$. It characterizes the distribution of the b-quark momentum inside the B meson and is usually parametrized by the Peterson form [4],

$$f(x) = N_\epsilon \frac{x(1-x)^2}{[(1-x)^2 + \epsilon x]^2}, \tag{3}$$

where ϵ is a free parameter and N_ϵ is determined so that $f(x)$ is normalized to 1. It is well known that the FF for the transition $b \to B$ peaks at large x. Since we expect a similar behaviour for the inverse transition $B \to b$, the Peterson ansatz should be well suited. Specifically, we adopt the value $\epsilon = 0.0126$, which was determined in the LO analysis of Ref. [8].

Using the formalism of Ref. [10], we obtain the following formula for the inclusive $B \to J/\psi + X$ decay width, differential in the J/ψ three-momentum $\boldsymbol{k'_\psi}$, in an arbitrary frame, where the B meson has three-momentum $\boldsymbol{P_B}$:

$$E_B E'_\psi \frac{d^3\Gamma'}{d^3k'_\psi} = \frac{G_F^2 M_\psi^3}{288\pi^2} |V_{cb}|^2 \left\{ \left[a - b + (a+b) \frac{M_B^2}{2M_\psi^2} (x_+ + x_-)^2 \right] [f(x_+) + f(x_-)] + (a+b) \frac{M_B^2}{2M_\psi^2} (x_+ + x_-)(x_+ - x_-) [f(x_+) - f(x_-)] \right\}, \tag{4}$$

where $E_B = \sqrt{\boldsymbol{P_B}^2 + M_B^2}$, $E_\psi = \sqrt{\boldsymbol{k_\psi}^2 + M_\psi^2}$, and

$$x_\pm = \frac{P_B \cdot k'_\psi \pm \sqrt{(P_B \cdot k'_\psi)^2 - M_B^2 M_\psi^2}}{M_B^2}. \tag{5}$$

Here, a prime is introduced to discriminate quantities referring to the system with finite $\boldsymbol{P_B}$ from their counterparts in the B rest frame. A similar formula applies to the inclusive $B \to \psi' + X$ decay.

Equation (4) is used in two ways. First, it is applied in the CLEO laboratory frame, where $|\boldsymbol{P_B}| = \sqrt{M_\Upsilon^2/4 - M_B^2} = 0.341$ GeV, after integration over the direction of $\boldsymbol{k'_\psi}$, to constrain the theoretical input entering a and b by comparison with the CLEO data [3]. For the prompt $B \to J/\psi + X$ decay, this was already done in Ref. [10]. A convenient alternative to doing the angular integration in the CLEO laboratory system is to carry it out in the B rest frame and then to perform a boost to the CLEO laboratory system. In the B rest frame, the decay width differential in $k_\psi = |\boldsymbol{k_\psi}|$ is easily obtained as [10]

$$\frac{d\Gamma}{dk_\psi} = \frac{G_F^2 M_\psi^3}{72\pi M_B} |V_{cb}|^2 \frac{k_\psi^2}{E_\psi} \left\{ \left[a - b + (a+b) \frac{M_B^2}{2M_\psi^2} (x_+ + x_-)^2 \right] [f(x_+) + f(x_-)] \right.$$
$$\left. + (a+b) \frac{M_B^2}{2M_\psi^2} (x_+ + x_-)(x_+ - x_-) [f(x_+) - f(x_-)] \right\}, \tag{6}$$

where $x_\pm$ is now given by

$$x_\pm = \frac{E_\psi \pm k_\psi}{M_B}. \tag{7}$$

Here, k_ψ varies in the interval $0 \le k_\psi \le k_{\psi,\max}$, where

$$k_{\psi,\max} = \frac{M_B^2 - M_\psi^2}{2M_B}. \tag{8}$$

In the CLEO laboratory frame, we then have

$$\frac{d\Gamma}{dk'_\psi} = \frac{M_B k'_\psi}{2P_B E'_\psi} \int_{k_1}^{k_2} \frac{dk_\psi}{k_\psi} \frac{d\Gamma}{dk_\psi}, \tag{9}$$

where

$$k_1 = \frac{|E_B k'_\psi - P_B E'_\psi|}{M_B}, \qquad k_2 = \min\left(\frac{E_B k'_\psi + P_B E'_\psi}{M_B}, k_{\psi,\max} \right). \tag{10}$$

Here, k'_ψ varies in the interval $\max(k'_-, 0) \le k'_\psi \le k'_+$, where

$$k'_\pm = \frac{P_B (M_B^2 + M_\psi^2) \pm E_B (M_B^2 - M_\psi^2)}{2M_B^2}. \tag{11}$$

Notice that $d\Gamma$ on the left-hand side of Eq. (9) refers to the B rest frame, so that integrating Eq. (9) over k'_ψ yields the proper $B \to J/\psi + X$ decay width.

The second application of Eq. (4) concerns the calculation of the $B \to J/\psi + X$ decay distribution in the component k'_L of the J/ψ three-momentum that is parallel to $\boldsymbol{P_B}$. For this purpose, we must integrate Eq. (4) over the orthogonal momentum component k'_T.

This can be directly done leading to

$$\frac{d\Gamma}{dk'_L} = \frac{G_F^2 M_\psi^3}{288\pi M_B}|V_{cb}|^2 \int_0^{k'^2_{T,\max}} \frac{dk'^2_T}{E'_\psi} \left\{ \left[a - b + (a+b)\frac{M_B^2}{2M_\psi^2}(x_+ + x_-)^2 \right] [f(x_+) + f(x_-)] \right.$$
$$\left. + (a+b)\frac{M_B^2}{2M_\psi^2}(x_+ + x_-)(x_+ - x_-)\,[f(x_+) - f(x_-)] \right\}, \tag{12}$$

where

$$k'^2_{T,\max} = \left(\frac{M_B^2 + M_\psi^2 + 2p_B k_L}{2E_B} \right)^2 - M_\psi^2 - k'^2_L \tag{13}$$

and $k'_- \le k'_L \le k'_+$. For most of our applications, $P_B = |\boldsymbol{P_B}| \gg M_B$ is satisfied. In this limit, an asymptotic formula for $d\Gamma/dx$, where $x = k'_L/P_B$, can be derived. Defining $r = M_\psi^2/M_B^2$ and $t = k'^2_T/M_B^2$, we have

$$\frac{d\Gamma}{dx}(x, P_B) = \frac{G_F^2 M_B^3 M_\psi}{288\pi x}|V_{cb}|^2 \int_0^{(x-r)(1-x)} dt \left\{ \left[r(a-b) + \frac{a+b}{2}(x_+ + x_-)^2 \right] \right.$$
$$\left. \times\, [f(x_+) + f(x_-)] + \frac{a+b}{2}(x_+ - x_-)^2\,[f(x_+) - f(x_-)] \right\}, \tag{14}$$

where

$$x_\pm = \frac{1}{2}\left(x + \frac{r+t}{x} \pm \sqrt{\left(x + \frac{r+t}{x} \right)^2 - 4r} \right), \tag{15}$$

and $r \le x \le 1$. An alternative way of calculating the distribution in Eq. (12) is to transform the k'_T integration into an integration over k_ψ in the B rest frame, in a way similar to Eq. (9). This leads to

$$\frac{d\Gamma}{dk'_L} = \frac{M_B}{2E_B} \int_{k_{\psi,\min}}^{k_{\psi,\max}} \frac{dk_\psi}{k_\psi} \frac{d\Gamma}{dk_\psi}, \tag{16}$$

where $d\Gamma/dk_\psi$ and $k_{\psi,\max}$ are given in Eqs. (6) and (8), respectively, and

$$k_{\psi,\min} = \frac{|E_B k'_L - P_B m'_L|}{M_B}, \tag{17}$$

with $m'_L = \sqrt{k'^2_L + M_\psi^2}$.

As already mentioned in Sect. 2, we incorporate the $B \to \psi + X$ decay in our calculation of inclusive B hadroproduction by defining effective FF's for the transition of the partons i that come out of the hard scattering to the ψ mesons as

$$D_{i\to\psi}(x, M_f^2) = \int_x^1 dz\, D_{i\to B}\left(\frac{x}{z}, M_f^2 \right) \frac{1}{\Gamma_B} \frac{d\Gamma}{dz}(z, P_B), \tag{18}$$

where $D_{i\to B}(x, M_f^2)$ are the nonperturbative FF's determined in Ref. [8], $\Gamma_B = 1/\tau_B$ is the total B decay width, and $d\Gamma(x, P_B)/dx$ is obtained from Eqs. (12) or (16). For

given ψ transverse momentum p_T and rapidity y, P_B in Eq. (18) is given by $P_B = \sqrt{p_T^2 + m_T^2 \sinh^2 y}/z$, where m_T is the ψ transverse mass. For reasons explained above, we choose the factorization scale to be $M_f = 2\xi m_T$. In our numerical analysis, we use the B^+/B^0 average values $M_B = 5.2791$ GeV and $\tau_B = 1.61$ ps [13] for the B mass and lifetime, respectively.

In the remainder of this section, we discuss the decays $B \to \chi_{cJ} + X$, with $J = 0, 1, 2$, within the NRQCD framework. They were not considered in Ref. [10]. They contribute via radiative feed-down to the yield of J/ψ mesons from b-hadron decay measured at the Tevatron and must, therefore, be included in our analysis. We find that Eq. (1) and the subsequent equations derived from it carry over to these cases if we substitute everywhere ψ by χ_{cJ}, insert

$$\begin{aligned}
a &= (C_+ + C_-)^2 \frac{\langle \mathcal{O}^{\chi_{c0}}[\underline{8}, {}^3S_1] \rangle}{2m_c^2}, \\
a &= (2C_+ - C_-)^2 \frac{2 \langle \mathcal{O}^{\chi_{c0}}[\underline{1}, {}^3P_0] \rangle}{m_c^4} + (C_+ + C_-)^2 \frac{3 \langle \mathcal{O}^{\chi_{c0}}[\underline{8}, {}^3S_1] \rangle}{2m_c^2}, \\
a &= (C_+ + C_-)^2 \frac{5 \langle \mathcal{O}^{\chi_{c0}}[\underline{8}, {}^3S_1] \rangle}{2m_c^2},
\end{aligned} \tag{19}$$

for $J = 0, 1, 2$, respectively, and put $b = 0$ in all three cases.

4 Nonperturbative charmonium matrix elements

In this section, we determine the leading NRQCD colour-octet matrix elements of the J/ψ, ψ', and χ_{cJ} mesons from fits to the CDF data of their prompt hadroproduction [1], imposing the requirement that the branching fractions of the inclusive B decays into these charmonium states, calculated as described in Sect. 3, agree with the CLEO results [3] whenever this is possible. This complements our previous analysis [21], where we determined the J/ψ and χ_{cJ} colour-octet matrix elements from the CDF data [1] alone.

We start by repeating the J/ψ analysis of Ref. [21] for the ψ' mesons. We extract $\left\langle \mathcal{O}^{\psi'}[\underline{1}, {}^3S_1] \right\rangle$ from the measured $\psi' \to \mu^+\mu^-$ decay width [13] using the QCD-improved formula (3) of Ref. [21]. We then determine the leading colour-octet matrix elements from the CDF data sample of prompt ψ' hadroproduction [1], which contains 5 data points. Similarly to the J/ψ analysis reported in Ref. [21], we obtain $\left\langle \mathcal{O}^{\psi'}[\underline{8}, {}^3S_1] \right\rangle$ from the upper part of the p_T spectrum (last 2 data points) working in the fragmentation picture, where the $c\bar{c}$ bound state is created from a single high-energy gluon, charm quark or antiquark which is close to its mass shell. In a second step, we extract the linear combination

$$M_r^{\psi'} = \left\langle \mathcal{O}^{\psi'}[\underline{8}, {}^1S_0] \right\rangle + \frac{r}{m_c^2} \left\langle \mathcal{O}^{\psi'}[\underline{8}, {}^3P_0] \right\rangle, \tag{20}$$

from the lower part of the p_T spectrum (first 4 data points) adopting the fusion picture, where the $c\bar{c}$ bound state is formed within the primary hard-scattering process. Here,

Table 1: Values of the J/ψ and ψ' matrix elements resulting from the minimum-χ^2 fits to the CDF data [1]. M_r^ψ is defined in Eq. (20).

ψ	J/ψ	ψ'
$\left\langle \mathcal{O}^\psi[\underline{1}, {}^3S_1] \right\rangle$	$(7.63 \pm 0.54) \cdot 10^{-1}$ GeV^3	$(4.40 \pm 0.43) \cdot 10^{-1}$ GeV^3
$\left\langle \mathcal{O}^\psi[\underline{8}, {}^3S_1] \right\rangle$	$(3.94 \pm 0.63) \cdot 10^{-3}$ GeV^3	$(6.20 \pm 0.95) \cdot 10^{-3}$ GeV^3
M_r^ψ	$(6.52 \pm 0.67) \cdot 10^{-2}$ GeV^3	$(1.79 \pm 0.51) \cdot 10^{-2}$ GeV^3
r	3.47	2.56
$\chi^2_{\rm DF}$ fus.	5.97/10	1.00/4
$\chi^2_{\rm DF}$ fra.	1.53/2	0.03/2
$\chi^2_{\rm DF}$ tot.	7.49/12	1.03/6

r is chosen in such a way that the superposition of these two channels is insensitive to precisely how they are weighted relative to each other. The results obtained with set CTEQ4L [17] of proton PDF's are listed in Table 1 together with our previous LO results for J/ψ mesons [21]. Our result for $M_r^{\psi'}$ agrees very well with the value $M_3^{\psi'} = (1.8 \pm 0.6) \cdot 10^{-2}$ GeV^3 found by Cho and Leibovich [22] from a fit to earlier CDF data, while our result for $\left\langle \mathcal{O}^{\psi'}[\underline{8}, {}^3S_1] \right\rangle$ is somewhat larger than their value $\left\langle \mathcal{O}^{\psi'}[\underline{8}, {}^3S_1] \right\rangle = (4.6 \pm 1.0) \cdot 10^{-3}$ GeV^3. Figure 1 illustrates, for the fusion picture, how the theoretical cross section of prompt ψ' hadroproduction compares with the corresponding CDF data [1] and how it is decomposed into its colour-singlet and colour-octet components. The total cross section in the fragmentation picture, which is complementary to the fusion picture, is not shown in Fig. 1 because it would be hardly distinguishable from the solid line. It is almost entirely due to the $[\underline{8}, {}^3S_1]$ channel, while the $[\underline{1}, {}^3S_1]$ contribution is approximately down by a factor of 60. The goodness of the fits in the fusion and fragmentation pictures is measured in terms of the χ^2 per degree of freedom, $\chi^2_{\rm DF}$. These values and their combinations are also given in Table 1.

As is well known [22], prompt hadroproduction of J/ψ and ψ' mesons is rather insensitive to the individual values of $\left\langle \mathcal{O}^\psi[\underline{8}, {}^1S_0] \right\rangle$ and $\left\langle \mathcal{O}^\psi[\underline{8}, {}^3P_0] \right\rangle$ as long as M_r^ψ is kept fixed. This is very different for their production from B decay. This circumstance may be exploited in order to separately fix $\left\langle \mathcal{O}^\psi[\underline{8}, {}^1S_0] \right\rangle$ and $\left\langle \mathcal{O}^\psi[\underline{8}, {}^3P_0] \right\rangle$ using the CLEO data [3]. We choose to do this by adjusting the NRQCD results for the $B \to \psi + X$ branching fractions so that they agree with the measured values. The outcome and the $\chi^2_{\rm DF}$ values achieved are summarized in Table 2. The fact that the CLEO data favour negative values of $\left\langle \mathcal{O}^{J/\psi}[\underline{8}, {}^3P_0] \right\rangle$ was already observed in Ref. [10]. The ψ' case was not considered there. The resulting $B \to \psi + X$ differential branching fractions $(1/\Gamma_B) d\Gamma/dk'_\psi$ for $\psi = J/\psi, \psi'$ are compared with the CLEO data in Figs. 2(a) and (b), respectively.

An alternative criterion for determining $\left\langle \mathcal{O}^\psi[\underline{8}, {}^1S_0] \right\rangle$ and $\left\langle \mathcal{O}^\psi[\underline{8}, {}^3P_0] \right\rangle$ is to minimize the χ^2 values of the theoretical decay spectrum with the experimental data. This leads

Table 2: Decompositions of M_r^ψ ($\psi = J/\psi, \psi'$) from Table 1 into $\left\langle \mathcal{O}^\psi[\underline{8}, {}^1S_0] \right\rangle$ and $\left\langle \mathcal{O}^\psi[\underline{8}, {}^3P_0] \right\rangle$ obtained by requiring that the NRQCD values of $B(B \to \psi + X)$ for prompt ψ production through B decay agree with the CLEO data [3]. The resulting values of $\chi^2_{\rm DF}$ are also given.

ψ	J/ψ	ψ'
$\left\langle \mathcal{O}^\psi[\underline{8}, {}^1S_0] \right\rangle$	$1.45 \cdot 10^{-1}$ GeV^3	$-9.66 \cdot 10^{-3}$ GeV^3
$\left\langle \mathcal{O}^\psi[\underline{8}, {}^3P_0] \right\rangle$	$-5.51 \cdot 10^{-2}$ GeV^5	$2.58 \cdot 10^{-2}$ GeV^5
$B(B \to \psi + X)$ (prompt)	0.800%	0.340%
$\chi^2_{\rm DF}$	103/20	16.5/8

Table 3: Same as in Table 2, but from minimum-χ^2 fits to the CLEO data [3].

ψ	J/ψ	ψ'
$\left\langle \mathcal{O}^\psi[\underline{8}, {}^1S_0] \right\rangle$	$2.23 \cdot 10^{-1}$ GeV^3	$1.26 \cdot 10^{-3}$ GeV^3
$\left\langle \mathcal{O}^\psi[\underline{8}, {}^3P_0] \right\rangle$	$-1.09 \cdot 10^{-1}$ GeV^5	$1.56 \cdot 10^{-2}$ GeV^5
$B(B \to \psi + X)$ (prompt)	0.684%	0.282%
$\chi^2_{\rm DF}$	93.5/20	13.4/8

to the results shown in Table 3. We observe that the $B \to J/\psi + X$ and $B \to \psi' + X$ branching fractions are reduced by 15% and 17% relative to Table 2, while the quality of the fits is only marginally improved. From the sign flip of $\left\langle \mathcal{O}^{\psi'}[\underline{8}, {}^1S_0] \right\rangle$ we conclude that this matrix element is not very well constrained from the CLEO data. On the other hand, its value in Table 3 is very small.

We remark that our fits to the CLEO data have bad $\chi^2_{\rm DF}$ values. From Figs. 2(a) and (b), we observe that the data both at small and large J/ψ momenta are not fitted well. At large J/ψ momentum, the spectrum is influenced by contributions from the K, K^*, and higher K^* resonances, which can only be included in an average way by our approach. We think that the exact shape of the J/ψ spectrum is not relevant after the boost to the Tevatron laboratory frame. Of importance, however, is the absolute normalization of the spectrum, since the final result is directly proportional to it. Therefore, the fit procedure leading to Table 2, which is faithful in the experimental normalization, should be preferred, and we use the results of Table 2 in the remainder of this paper.

We now turn to the $B \to \chi_{cJ} + X$ decays. The relevant matrix elements for their description in the NRQCD framework are $\langle \mathcal{O}^{\chi_{c0}}[\underline{1}, {}^3P_0] \rangle$ and $\langle \mathcal{O}^{\chi_{c0}}[\underline{8}, {}^3S_1] \rangle$. For our analysis, we adopt the value $\langle \mathcal{O}^{\chi_{c0}}[\underline{1}, {}^3P_0] \rangle = (8.80 \pm 2.13) \cdot 10^{-2}$ GeV^5 from Ref. [23], where is was determined from the measured hadronic decay widths of the χ_{cJ} mesons. Using

the central value of this result, we then find $\langle \mathcal{O}^{\chi_{c0}}[\underline{8}, {}^3S_1] \rangle = (1.39 \pm 0.17) \cdot 10^{-3}$ GeV^3 from a LO fit to the CDF data on prompt χ_{cJ} hadroproduction [1]. Using the NRQCD formalism described in Sect. 3 with this input, we evaluate the $B \to \chi_{cJ} + X$ branching fractions for $J = 0, 1, 2$ to be $8.73 \cdot 10^{-5}$, $5.38 \cdot 10^{-4}$, and $3.90 \cdot 10^{-4}$, respectively. These values are incompatible with the CLEO results, $B(B \to \chi_{c1} + X) = (4.0 \pm 0.6 \pm 0.4) \cdot 10^{-3}$ and $B(B \to \chi_{c2} + X) = (2.5 \pm 1.0 \pm 0.3) \cdot 10^{-3}$ [3], where the first error is statistical and the second systematic. $B \to \chi_{c0} + X$ decays were not observed by CLEO. Obviously, the CDF data on $p\bar{p} \to \chi_{cJ} + X$ and the CLEO data on $B \to \chi_{cJ} + X$ cannot be simultaneously interpreted to LO in the NRQCD framework. The inclusion of the NLO corrections to the $B \to \chi_{cJ} + X$ decay width does not remove this discrepancy [24]. In want of a theoretically satisfactory solution to this problem, we choose a purely phenomenological description. We calculate the momentum spectrum of the J/ψ mesons from B decay via the χ_{cJ} states to LO in NRQCD, using the above matrix elements, an average χ_{cJ}-meson mass of 3.495 GeV, and the values of $B(\chi_{cJ} \to J/\psi + \gamma)$ from Ref. [13], and adjust its normalization in accordance with the CLEO result, to be $(1.3 \pm 0.2) \cdot 10^{-3}$ [3]. Without this normalization factor, we would have $\sum_{J=0}^{2} B(B \to \chi_{cJ} + X) B(\chi_{cJ} \to J/\psi + \gamma) = 2.05 \cdot 10^{-4}$. The CLEO Collaboration did not specify experimental data on the momentum spectrum of the J/ψ mesons originating from the χ_{cJ} states. However, they published the measured decay spectrum for the combined J/ψ sample, including prompt production and feed-down from χ_{c1}, χ_{c2}, and ψ' states. In Fig. 2(c), these data are compared with the superposition of our NRQCD results. Notice that both experimental and theoretical results have the same normalization.

5 Charmonium production from *b*-hadron decay in $p\bar{p}$ collisions

In this section, we present our predictions for the inclusive production of J/ψ and ψ' mesons originating from b-hadron decay in $p\bar{p}$ collisions at the Tevatron and compare them with available CDF [1] and D0 [15] data. As described in Sect. 3, the cross section of this process emerges from the one of inclusive b-hadron production by convolution with the longitudinal-momentum distribution of the J/ψ and ψ' mesons from b-hadron decay appropriately boosted along the b-hadron flight direction. In Fig. 3, we investigate how the $B \to J/\psi + X$ branching fraction $(1/\Gamma_B) d\Gamma(x, P_B)/dx$ differential in $x = k'_L/P_B$, as given by Eqs. (12) or (16), is distorted by a boost to the frame where the B meson has nonvanishing three-momentum P_B. Specifically, we consider the cases $P_B = 5$, 10, and 20 GeV. For comparison, also the asymptotic line shape according to Eq. (14), which refers to the infinite-momentum frame, is shown. We observe that the finite-P_B results rapidly converge towards the asymptotic form. In order to obtain the effective $i \to J/\psi$ FF's via B decay, we need to convolute the $B \to J/\psi + X$ decay distribution shown in Fig. 3 with our $i \to B$ FF's [8] according to Eq. (18).

Having fixed all relevant input from fits to the OPAL data on $e^+e^- \to B + X$ [7], the CDF data on $p\bar{p} \to \psi + X$ via prompt production [1], and the CLEO data on $B \to \psi + X$

[3], we are now in a position to make absolute predictions for charmonium production via b-hadron decay in $p\bar{p}$ collisions. In Figs. 4(a) and (b), we consider J/ψ production, summing over the prompt channel and the feed-down channels via χ_{cJ} and ψ' states. In Fig. 4(a), the p_T distribution $d\sigma/dp_T$ measured by CDF [1] in the central region of the detector, for $|y| < 0.6$, is compared with our LO and NLO predictions based on the CTEQ4 [17] and MRST [18] PDF's and scale choice $\xi = 1$. In Fig. 4(b), the ξ dependence of these predictions is analyzed for three representative values of p_T. As a rule, the theoretical uncertainty may be estimated from three criteria: (i) the difference between the LO and NLO predictions; (ii) the shift due to scale variations; and (iii) the variation between different PDF sets. All these points may be studied with the help of Figs. 4(a) and (b). We find good agreement with the experimental data, especially in the upper p_T range, where the theoretical uncertainty is smallest. As expected, the NLO results are there more stable under scale variations than the LO ones. At the lower end of the p_T spectrum, the NLO results undershoot the data, but exhibit sizeable normalization uncertainties. The CTEQ and MRST PDF's lead to very similar results, except at very low p_T. In Fig. 5, the J/ψ analysis of Fig. 4(a) is repeated for ψ' mesons. Here, the agreement between experimental data and NLO predictions is also good at low p_T, where the theoretical uncertainty is largest.

The CDF [1] and D0 [15] Collaborations also published their full data samples on J/ψ production without discriminating between prompt production, feed-down from charmonium states with higher masses, and b-hadron decay. These cross sections are both differential in p_T, but are complementary in the sense that the CDF data are integrated over the central region, with $|y| < 0.6$, while the D0 data are sampled in the forward and backward directions, with $2.5 < |y| < 3.7$. In Figs. 6(a) and (b), we compare these data with our predictions obtained from the formalism explained here and in Ref. [21] with the nonperturbative charmonium matrix elements determined in Sect. 4. We work at LO using the CTEQ4L PDF's [17]. Apart from the total contributions, also the partial contributions due to prompt production, feed-down from χ_{cJ} mesons, feed-down from ψ' mesons, and b-hadron decay (summing over the prompt and feed-down channels) are shown. In the case of CDF, there is good agreement over the full p_T range considered. This is not surprising because the contributing matrix elements were actually determined from the prompt J/ψ, χ_{cJ}, and ψ' data samples taken in the same experiment. Furthermore, we already know from Fig. 4(a) that the predicted b-hadron decay contribution agrees well with the CDF data. So far, the D0 Collaboration did not present separate cross sections for the individual channels of J/ψ production. The agreement between their combined cross section and the theoretical prediction, which is essentially tuned to fit the CDF data, is remarkably good, except at the upper end of the p_T spectrum. In a way, Fig. 6(b) represents an indirect comparison between the CDF and D0 data on J/ψ production, which refer to different kinematic regimes. We notice that, at large p_T, the cross sections of the prompt and b-hadron channels are of the same order for the CDF central production [see Fig. 6(a)], whereas, in the case of D0 forward (backward) production, the prompt channel plays the dominant rôle [see Fig. 6(b)]. This means that the cross sections of these two channels have different rapidity dependences. This could

be checked experimentally if these cross sections were measured separately also in the forward (backward) direction.

6 Conclusions

We considered the hadroproduction in $p\bar{p}$ collisions of b hadrons which subsequently decay to charmonia and presented theoretical predictions for the p_T distribution of the latter. The formation of the b hadrons was described in the QCD-improved parton model with FF's fitted to e^+e^- data on B-meson production [8]. In want of detailed experimental information of the FF's of B_s mesons and Λ_b baryons, we approximately accounted for their contributions by appropriately adjusting the normalization of our B FF's [8]. The B decays to the various charmonium states were treated in NRQCD [10] with nonperturbative matrix elements determined from the CDF [1] and CLEO [3] data on prompt-charmonium production in $p\bar{p}$ collisions and B decay, respectively. In the case of the $B \to \chi_{cJ} + X$ decays, the NRQCD results for their branching fractions came out considerably smaller than the CLEO results [3], so that we had to include a phenomenological magnification factor. Furthermore, we assumed that the decays of B_s mesons and Λ_b baryons to charmonia, for which no data exist so far, can be described on the same footing as the B decays. We compared the CDF data on J/ψ and ψ' production from b-hadron decay [1] with our theoretical predictions and found good agreement. We estimated the theoretical uncertainty by comparing LO and NLO predictions, by scale variation, and by varying the PDF's and found that it was of order $\pm 25\%$ for $p_T \gtrsim 13$ GeV. We also compared the full CDF [1] and D0 [15] data samples on J/ψ production without distinguishing between prompt, feed-down, and b-hadron decay channels with our predictions. Again, we found good agreement. Since the CDF and D0 data refer to different ranges of rapidity, this may also be regarded as an indirect comparison between them.

ACKNOWLEDGMENTS

One of us (G.K.) is grateful to the Theory Group of the Werner-Heisenberg-Institut for the hospitality extended to him during a visit when this paper was prepared.

References

[1] CDF Collaboration, F. Abe *et al.*, Phys. Rev. Lett. **79**, 572 (1997); **79**, 578 (1997); T. Daniels, Ph. D. thesis, Massachusetts Institute of Technology (1997).

[2] P. Nason, S. Dawson, and R. K. Ellis, Nucl. Phys. **B303**, 607 (1988); **B327**, 49 (1989); for a review, see S. Frixione, M. L. Mangano, P. Nason, and G. Ridolfi, in *Heavy Flavors II*, edited by A. J. Buras and M. Lindner (World Scientific, Singapore, 1998), p. 609.

[3] CLEO Collaboration, R. Balest *et al.*, Phys. Rev. D **52**, 2661 (1995).

[4] C. Peterson, D. Schlatter, I. Schmitt, and P. M. Zerwas, Phys. Rev. D **27**, 105 (1983).

[5] J. Chrin, Z. Phys. C **36**, 163 (1987).

[6] B. A. Kniehl, M. Krämer, G. Kramer, and M. Spira, Phys. Lett. B **356**, 539 (1995).

[7] OPAL Collaboration, G. Alexander *et al.*, Phys. Lett. B **364**, 93 (1995).

[8] J. Binnewies, B. A. Kniehl, and G. Kramer, Phys. Rev. D **58**, 034016 (1998).

[9] CDF Collaboration, A. Laasanen *et al.*, Report No. FERMILAB-Conf-96/198-E (July 1996).

[10] W. F. Palmer, E. A. Paschos, and P. H. Soldan, Phys. Rev. D **56**, 5794 (1997).

[11] E. Braaten, K. Cheung, and T. C. Yuan, Phys. Rev. D **48**, R5049 (1993).

[12] C.-H. Chang and Y.-Q. Chen, Phys. Rev. D **49**, 3399 (1994).

[13] Particle Data Group, C. Caso *et al.*, Eur. Phys. J. C **3**, 1 (1998).

[14] G. T. Bodwin, E. Braaten, and G. P. Lepage, Phys. Rev. D **51**, 1125 (1995); **55**, 5853(E) (1997).

[15] D0 Collaboration, B. Abbott *et al.*, Phys. Rev. Lett. **82**, 35 (1999).

[16] F. M. Borzumati, B. A. Kniehl, and G. Kramer, Z. Phys. C **57**, 595 (1993), and papers cited therein.

[17] H. L. Lai, J. Huston, S. Kuhlmann, F. Olness, J. Owens, D. Soper, W. K. Tung, and H. Weerts, Phys. Rev. D **55**, 1280 (1997).

[18] A. D. Martin, R. G. Roberts, W. J. Stirling, and R. S. Thorne, Eur. Phys. J. C **4**, 463 (1998); Phys. Lett. B **443**, 301 (1998).

[19] J. Binnewies, B. A. Kniehl, and G. Kramer, Z. Phys. C **76**, 677 (1997).

[20] A. Ali and E. Pietarinen, Nucl. Phys. **B154**, 519 (1979); G. Altarelli, N. Cabibbo, G. Corbo, L. Maiani, and G. Martinelli, Nucl. Phys. **B208**, 365 (1982).

[21] B. A. Kniehl and G. Kramer, Eur. Phys. J. C **6**, 493 (1999).

[22] P. Cho and A. K. Leibovich, Phys. Rev. D **53**, 150 (1996); **53**, 6203 (1996).

[23] G. T. Bodwin, E. Braaten, and G. P. Lepage, Phys. Rev. D **46**, R1914 (1992).

[24] M. Beneke, F. Maltoni, and I.Z. Rothstein, Report No. CERN-TH/98-240, CMU-9805, and hep-ph/9808360 (August 1998).

FIGURE CAPTIONS

Figure 1: Fit to the CDF data on the inclusive hadroproduction of prompt ψ' mesons [1], which come in the form of $d\sigma/dp_T$ integrated over $|y| < 0.6$ as a function of p_T. Only the fusion results are shown.

Figure 2: Fit to the CLEO data on the production through B decay of (a) prompt J/ψ mesons, (b) ψ' mesons, and (c) J/ψ mesons including those from the feed-down of χ_{c1}, χ_{c2}, and ψ' mesons [3].

Figure 3: $B \to J/\psi + X$ (prompt) branching fraction differential in the J/ψ longitudinal momentum fraction relative to the B momentum P_B for various values of P_B. The result for $P_B = \infty$ is evaluated from Eq. (14).

Figure 4: The CDF data on the inclusive hadroproduction of b hadrons decaying to J/ψ mesons [1] are compared with LO and NLO predictions evaluated with CTEQ4 [17] and MRST [18] proton PDF's. (a) p_T dependence for scale choice $\xi = 1$ and (b) ξ dependence for selected values of p_T.

Figure 5: The CDF data on the inclusive hadroproduction of b hadrons decaying to ψ' mesons [1] are compared with LO and NLO predictions evaluated with CTEQ4 [17] and MRST [18] proton PDF's.

Figure 6: The (a) CDF [1] and (b) D0 [15] data on the inclusive hadroproduction of J/ψ mesons from all channels are compared with LO predictions evaluated with CTEQ4L [17] proton PDF's.

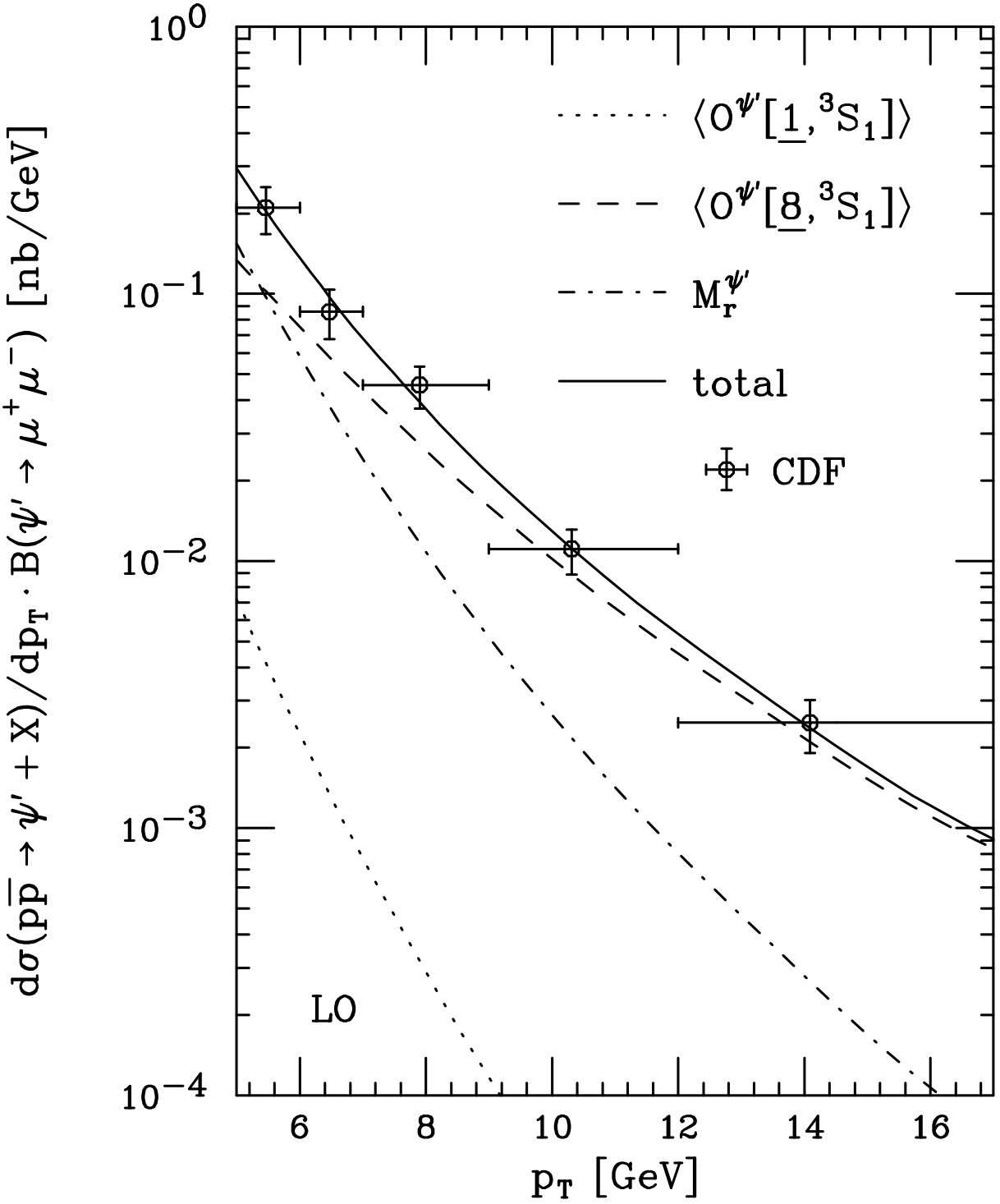
10^0
10^{-1}
10^{-2}
10^{-3}
10^{-4}
$d\sigma(p\bar{p} \to \psi' + X)/dp_T \cdot B(\psi' \to \mu^+\mu^-)$ [nb/GeV]
$\langle O^{\psi'}[1,^3S_1]\rangle$
$\langle O^{\psi'}[8,^3S_1]\rangle$
$M_r^{\psi'}$
total
CDF
LO
6
8
10
12
14
16
p_T [GeV]

Fig. 1

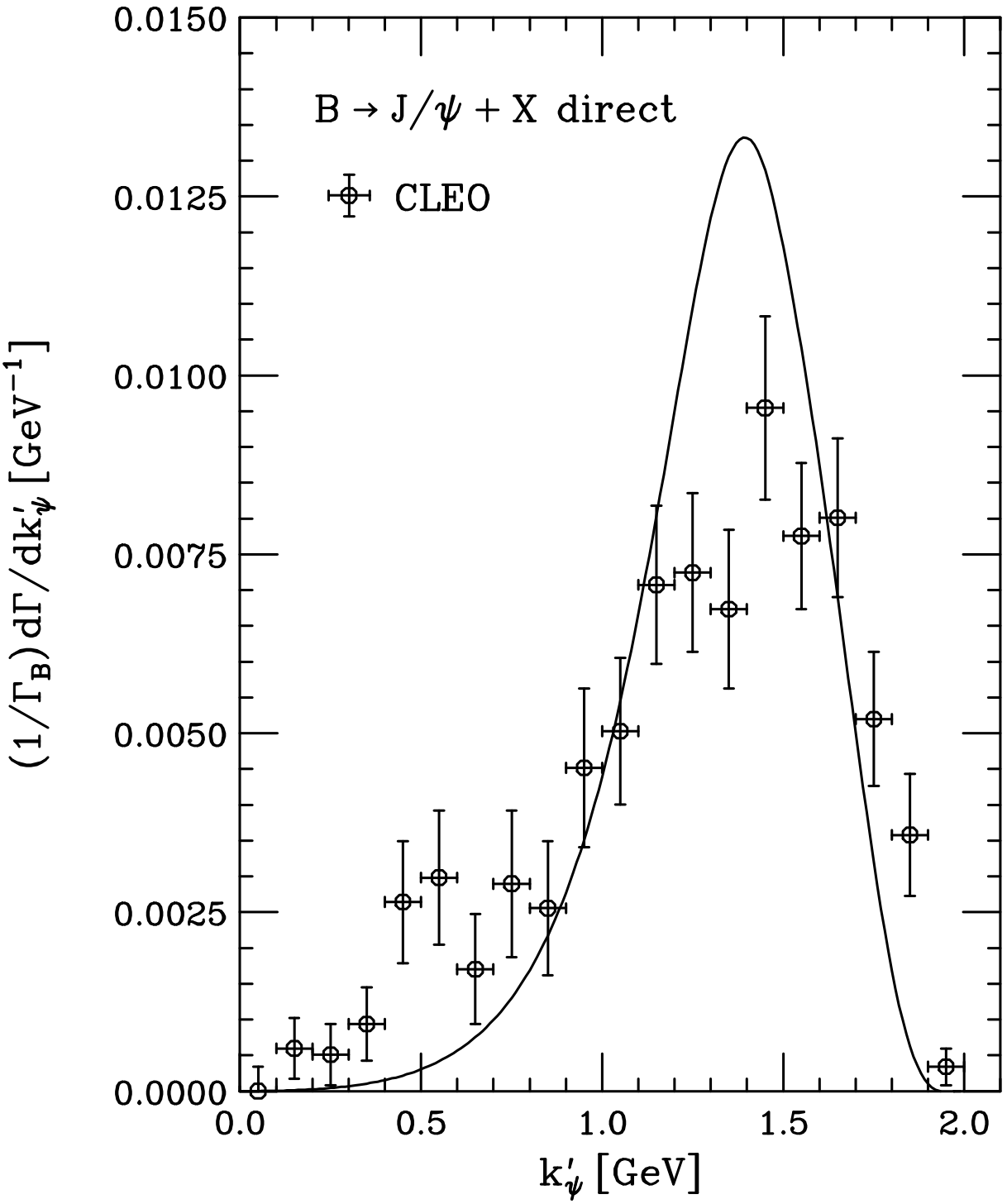
B → J/ψ + X direct
CLEO
0.0150
0.0125
0.0100
0.0075
0.0050
0.0025
0.0000
0.0
0.5
1.0
1.5
2.0
(1/Γ_B) dΓ/dk'_ψ [GeV^-1]
k'_ψ [GeV]

Fig. 2a

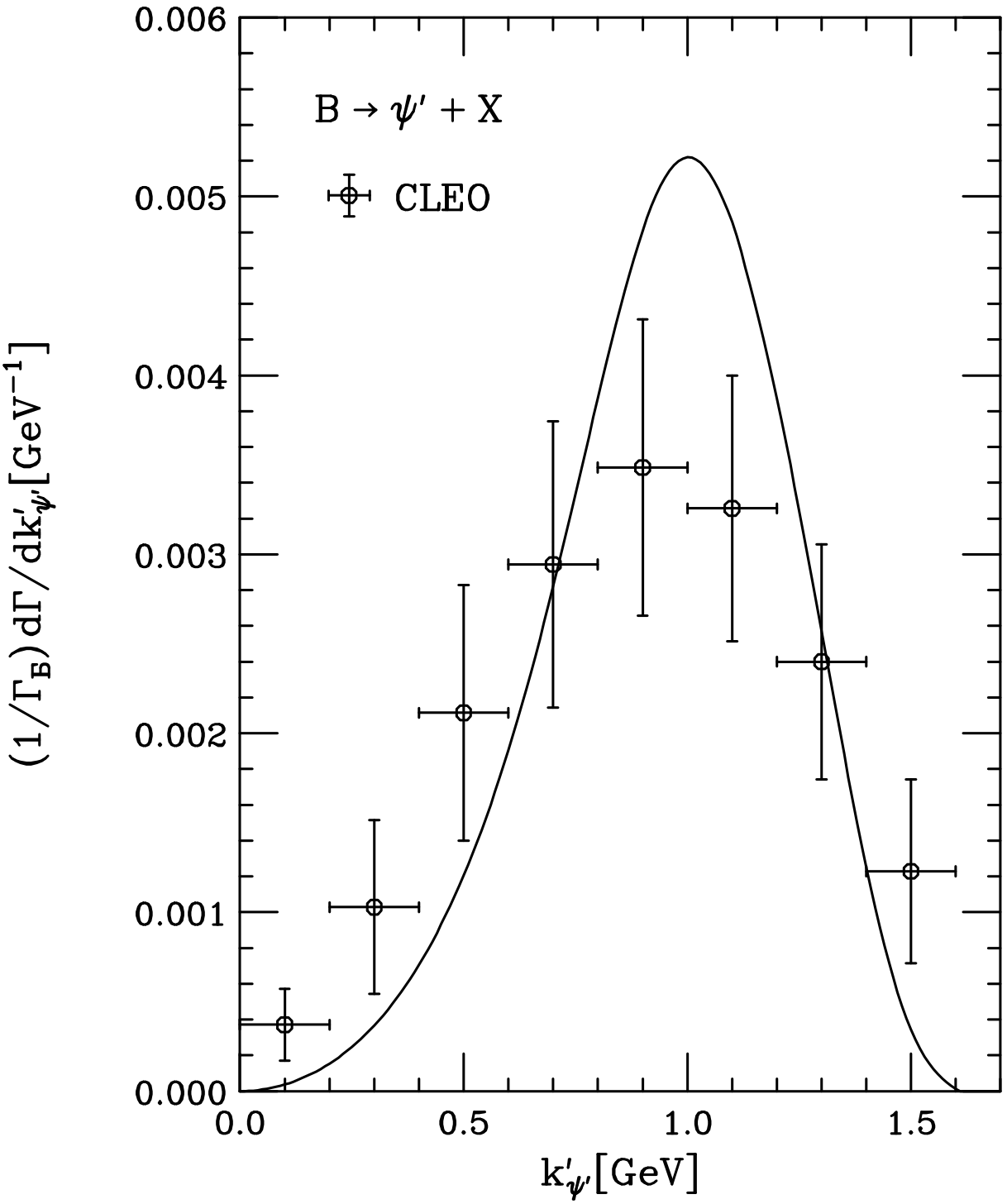
0.006
0.005
0.004
0.003
0.002
0.001
0.000
0.0
0.5
1.0
1.5
B → ψ′ + X
CLEO
(1/Γв) dΓ/dk′ψ′[GeV⁻¹]
k′ψ′[GeV]

Fig. 2b

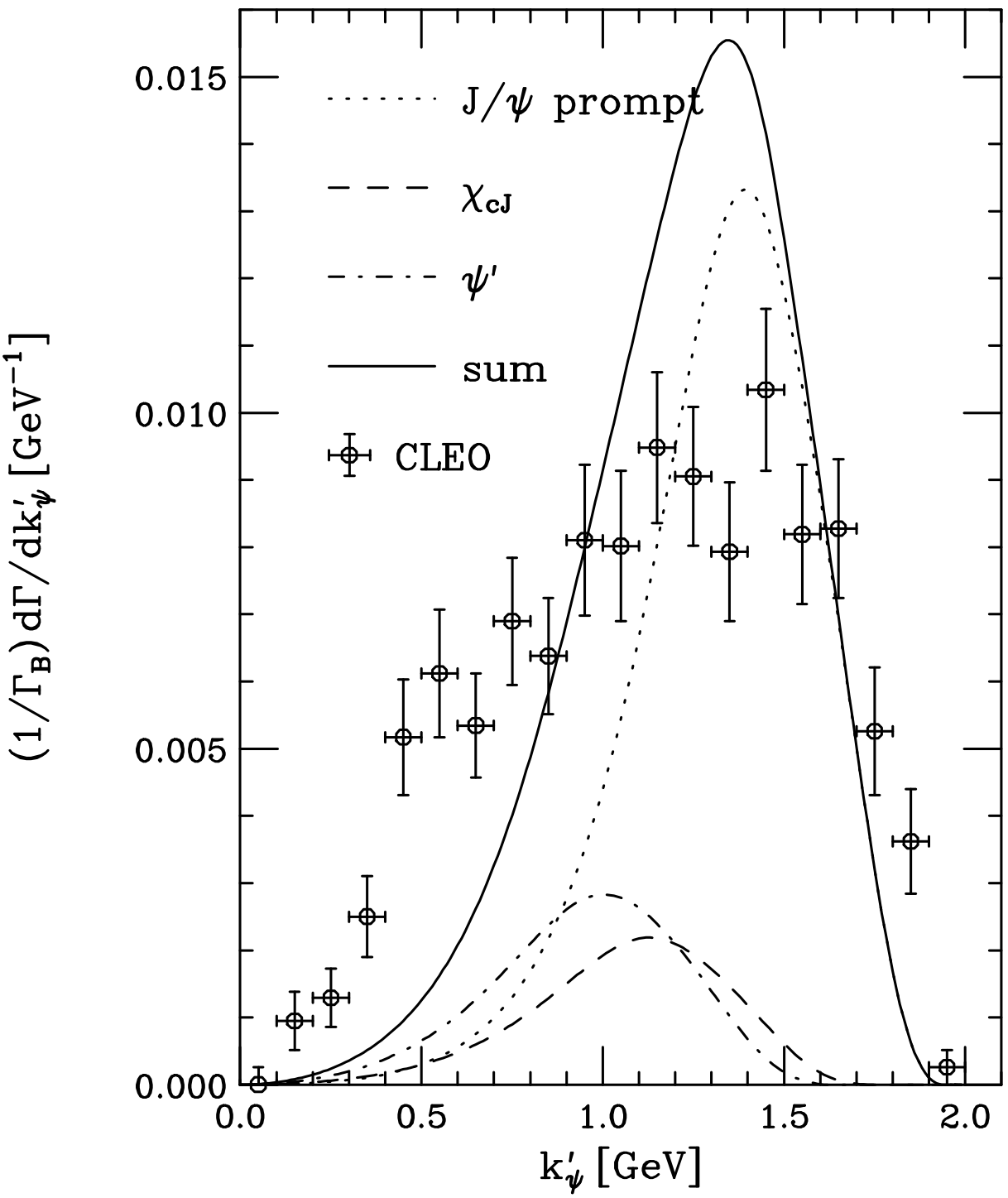
0.015
0.010
0.005
0.000
0.0
0.5
1.0
1.5
2.0
J/ψ prompt
χcJ
ψ'
sum
CLEO
(1/ΓB) dΓ/dk'ψ [GeV−1]
k'ψ [GeV]

Fig. 2c

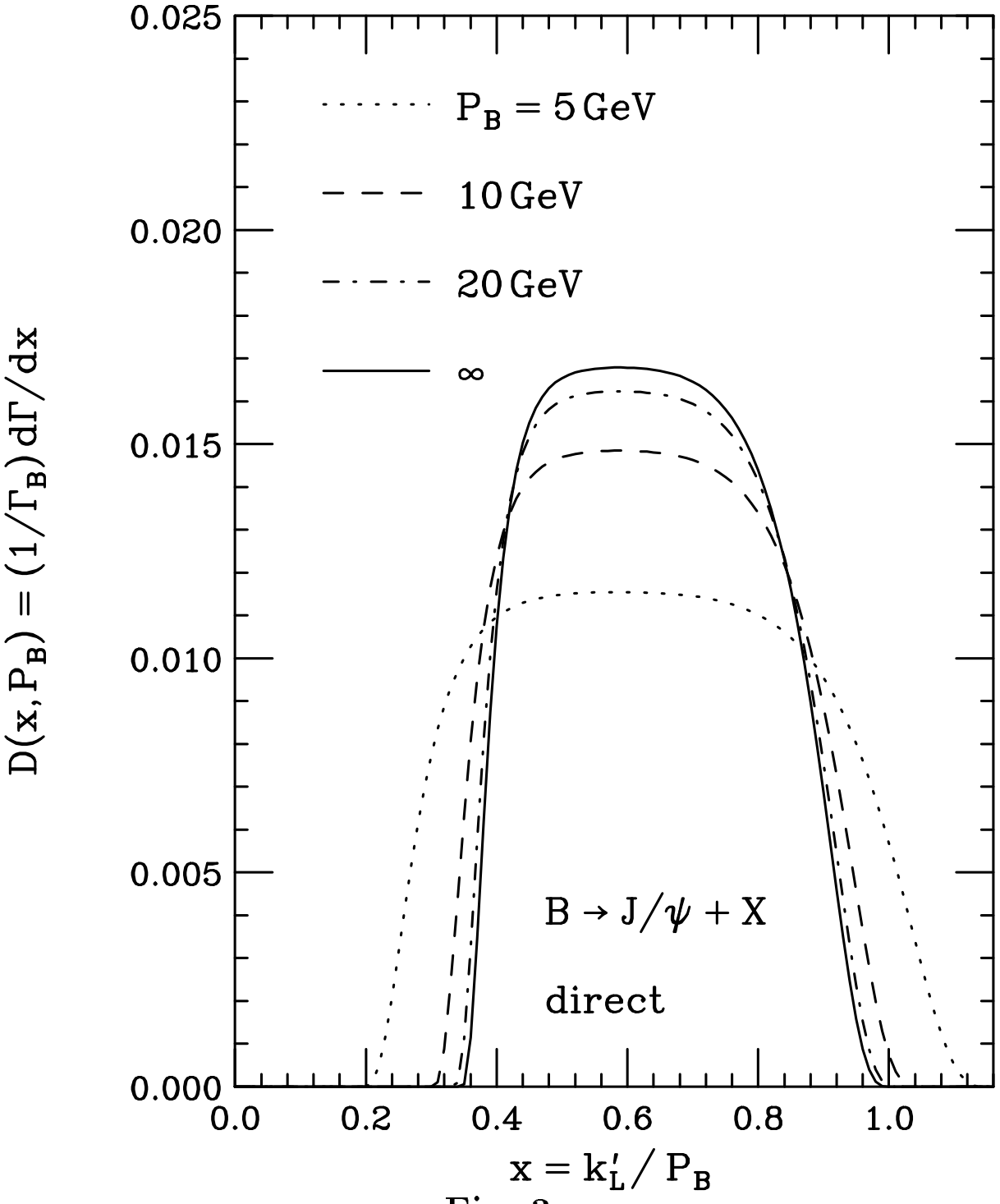
0.025
0.020
0.015
0.010
0.005
0.000
0.0
0.2
0.4
0.6
0.8
1.0
$P_B = 5\,GeV$
$10\,GeV$
$20\,GeV$
∞
$B \to J/\psi + X$
direct
$D(x, P_B) = (1/\Gamma_B)\, d\Gamma/dx$
$x = k'_L / P_B$

Fig. 3

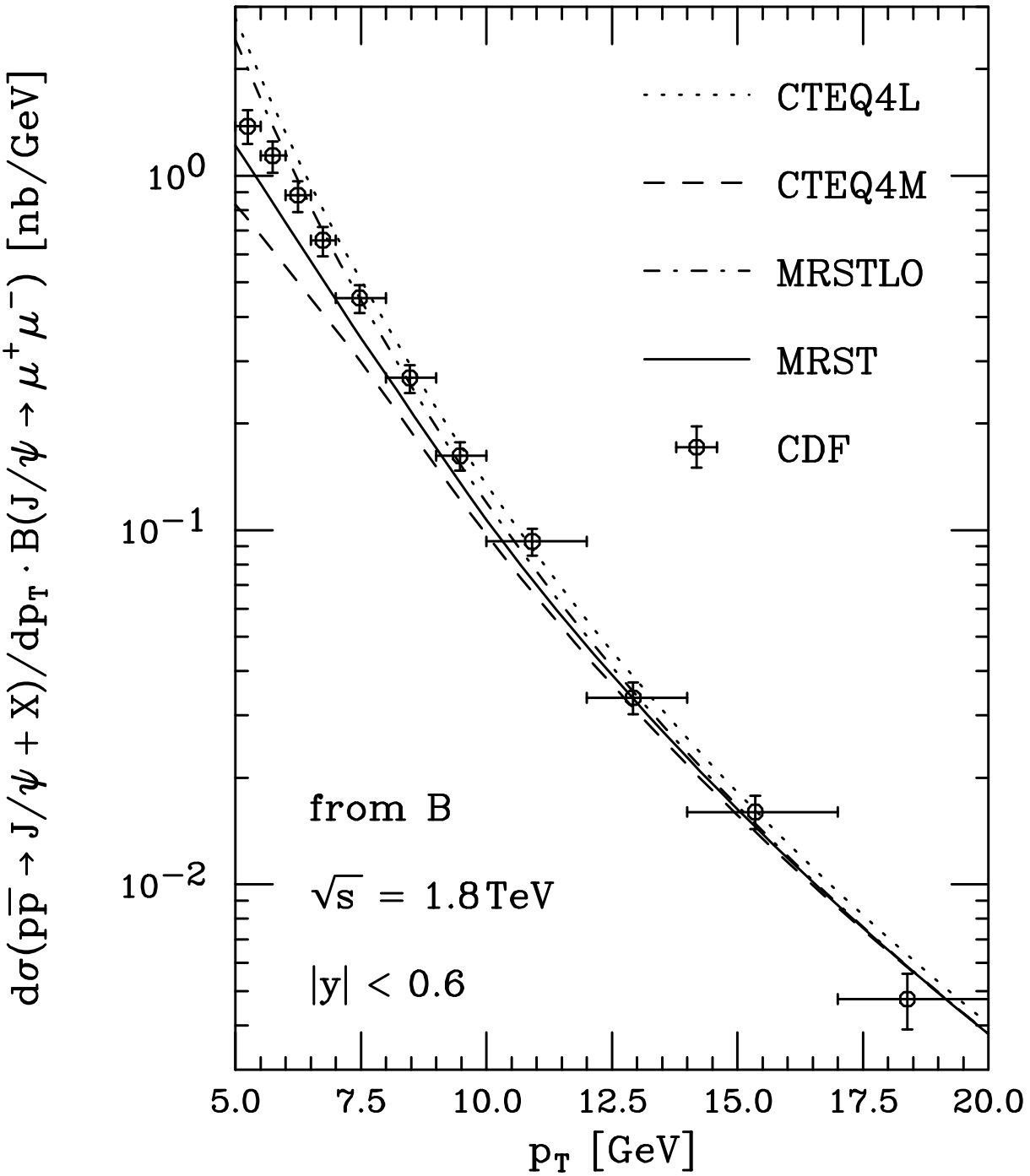
CTEQ4L
CTEQ4M
MRSTLO
MRST
CDF
from B
$\sqrt{s}$ = 1.8 TeV
|y| < 0.6
$d\sigma(p\bar{p} \to J/\psi + X)/dp_T \cdot B(J/\psi \to \mu^+\mu^-)$ [nb/GeV]
p_T [GeV]
10^0
10^{-1}
10^{-2}
5.0
7.5
10.0
12.5
15.0
17.5
20.0

Fig. 4a

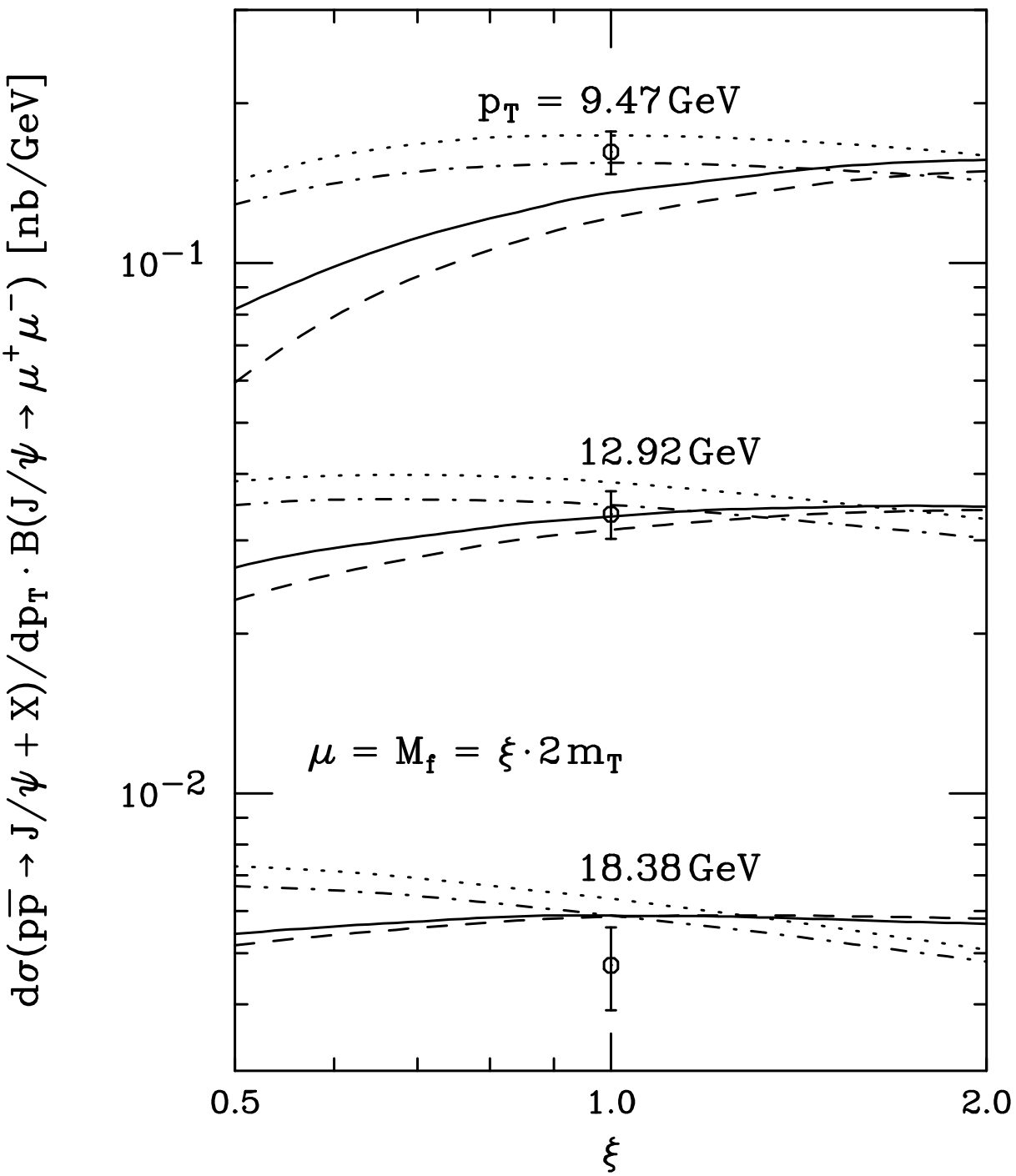
$p_T = 9.47\,GeV$
12.92 GeV
18.38 GeV
$\mu = M_f = \xi \cdot 2 m_T$
10^{-1}
10^{-2}
0.5
1.0
2.0
ξ
$d\sigma(p\bar{p} \to J/\psi + X)/dp_T \cdot B(J/\psi \to \mu^+\mu^-)$ [nb/GeV]

Fig. 4b

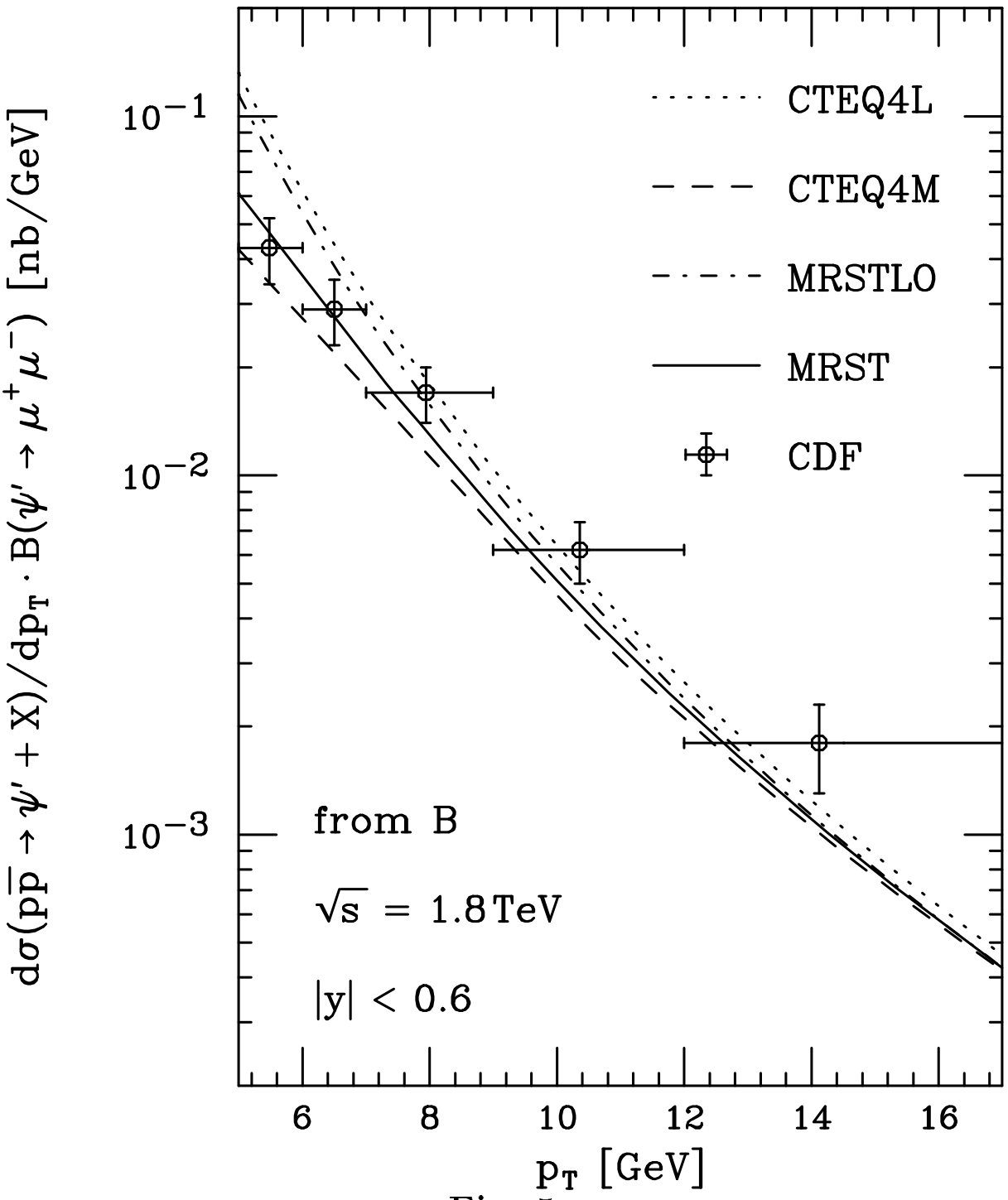
$d\sigma(p\bar{p} \to \psi' + X)/dp_T \cdot B(\psi' \to \mu^+\mu^-)$ [nb/GeV]
10^{-1}
10^{-2}
10^{-3}
CTEQ4L
CTEQ4M
MRSTLO
MRST
CDF
from B
$\sqrt{s}$ = 1.8 TeV
|y| < 0.6
6
8
10
12
14
16
p_T [GeV]

Fig. 5

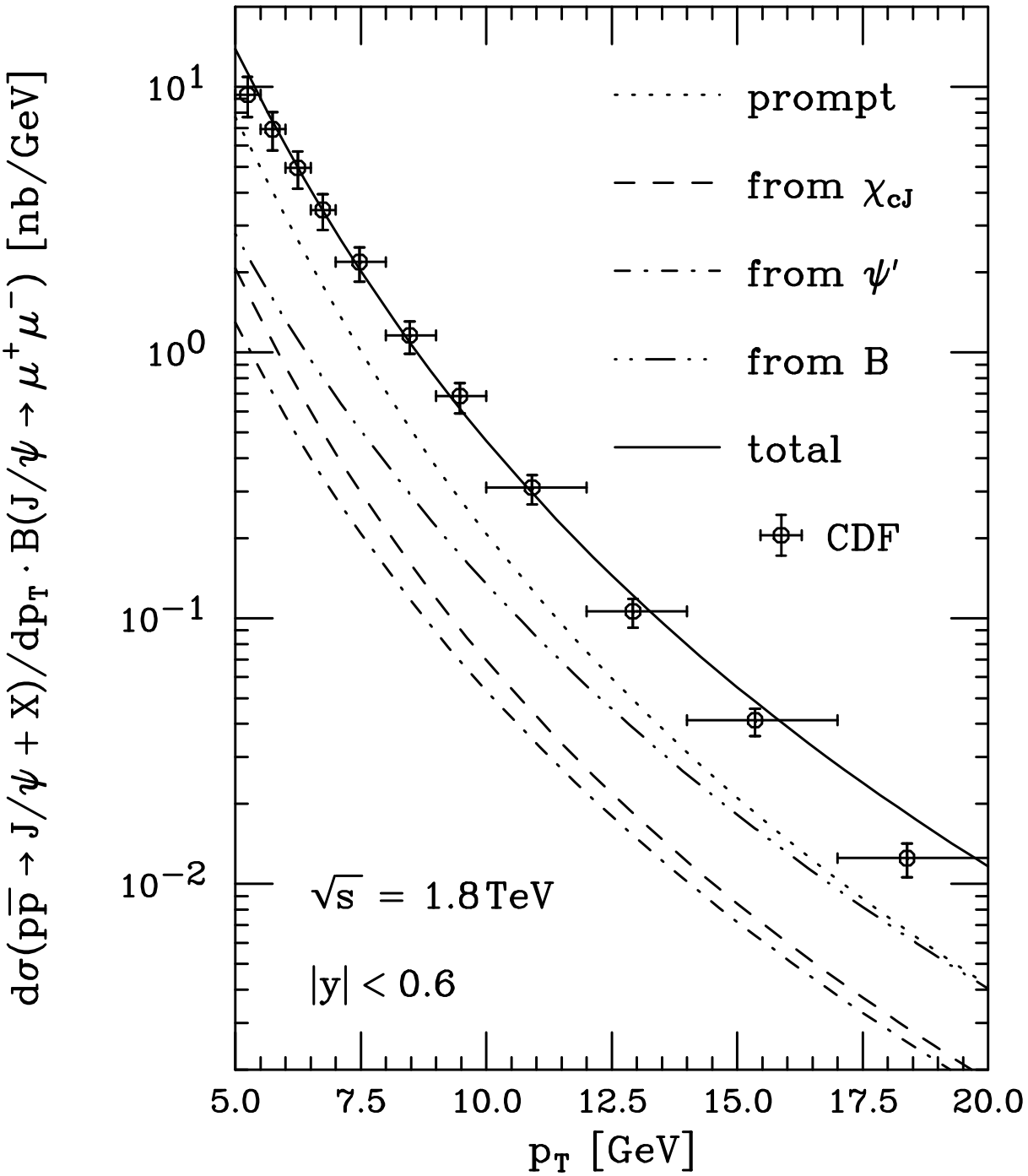
$d\sigma(p\bar{p} \to J/\psi + X)/dp_T \cdot B(J/\psi \to \mu^+\mu^-)$ [nb/GeV]
10^1
10^0
10^{-1}
10^{-2}
prompt
from χ_{cJ}
from ψ'
from B
total
CDF
$\sqrt{s}$ = 1.8 TeV
|y| < 0.6
5.0
7.5
10.0
12.5
15.0
17.5
20.0
p_T [GeV]

Fig. 6a

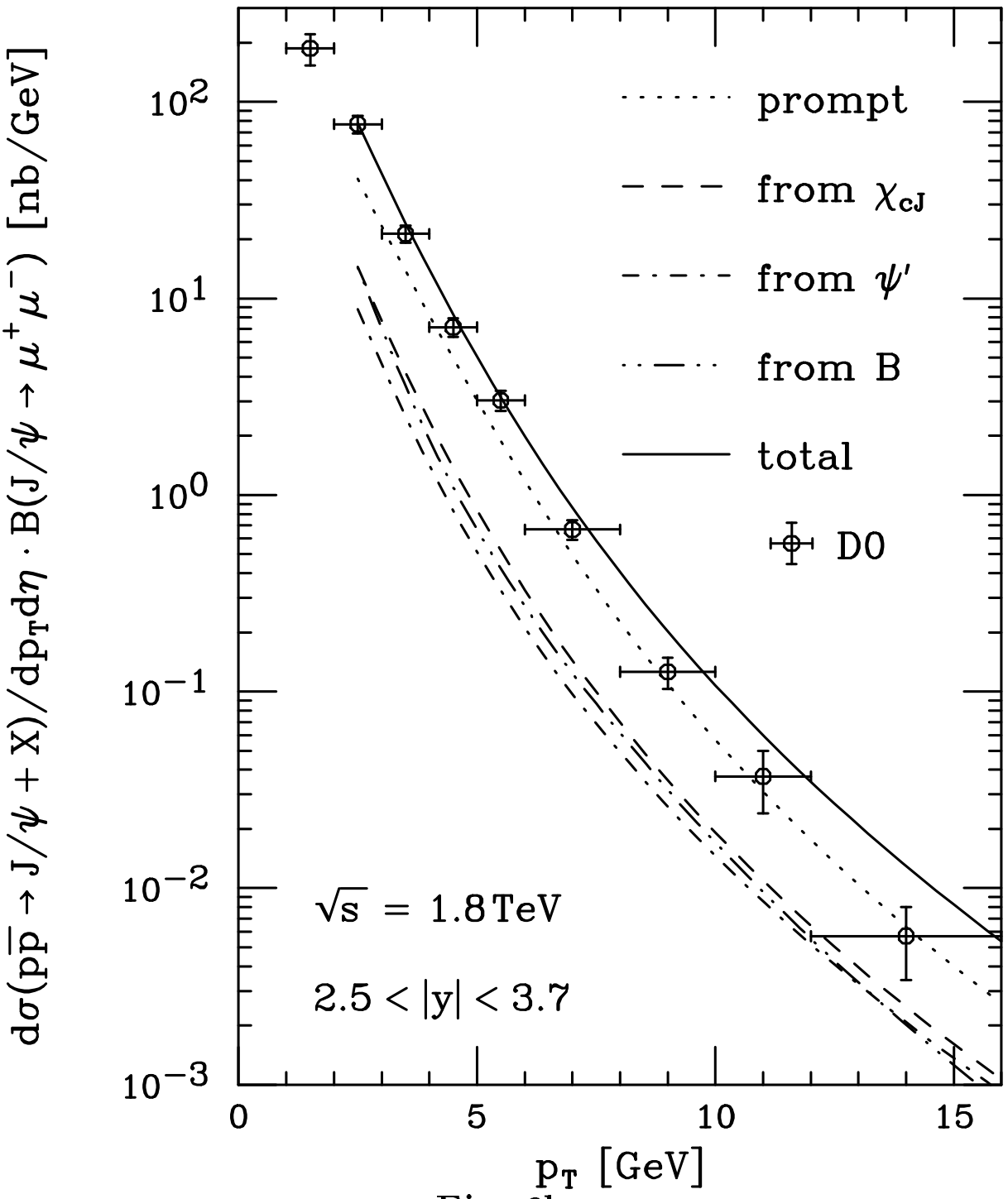
prompt
from χ_{cJ}
from ψ'
from B
total
D0
$\sqrt{s}$ = 1.8 TeV
2.5 < |y| < 3.7
$d\sigma(p\bar{p} \to J/\psi + X)/dp_T d\eta \cdot B(J/\psi \to \mu^+\mu^-)$ [nb/GeV]
p_T [GeV]
10^2
10^1
10^0
10^{-1}
10^{-2}
10^{-3}
0
5
10
15

Fig. 6b